**International Journal of Engineering Research**

**Sirte University**
**Faculty of Engineering**

Journal homepage: Scientific Journals (su.edu.ly)

# Design and Implementation of an Innovative Balun Configuration for Planar Antenna Use

*Younus A. Mohammed*[1]

*Sirte University, Sirte, Libya*
younus.mohammed@su.edu.ly

ARTICLE INFOR

*Article history:*

*Received 12 Jan 2024*

*Revised 19 Feb 2024*

*Accepted 25 Feb 2024*
*Available online:*

*1st April 2024*

ABSTRACT

The main parts of balanced circuits, including push-pull amplifiers, balanced mixers, frequency multipliers, and antennas, are baluns. Due to the increased integration of most of these applications, baluns must be inexpensive and of small size. This research paper presents a novel method for designing planar baluns. The approach begins by examining a symmetrical 4-port network features an open-circuit termination on one port, utilizing both even and odd mode stimulations. The suggested balun, supported by comprehensive design equations, showcases a completely balanced output and excellent input alignment, with measurement outcomes aligning closely with the simulated values.



**Keywords:** *balun planar lumped distributed even-odd mode*

## 1. Introduction

Low profile and inexpensive passive components are in high demand due to the rapid advancement of wireless communication technology. A balun, a crucial circuit component in balanced devices including frequency multipliers, push-pull amplifiers, antennas, and double-balanced mixers, is one of these fundamental parts. The main function of a balun is to align an imbalanced circuit configuration with a balanced one. At the balanced circuit, the signals have a 180-degree phase difference and are of equal magnitude over the relevant

frequencies. The other reason that baluns are used in RF and microwave circuits is for impedance matching between unbalanced and balanced ports. There are lumped, dispersed, or both lumped and distributed parts in the balun configurations. The dispersed baluns are made up of N segments of transmission lines [1]-[3]. A transmission line with a half wavelength is the most basic distributed balun. This balun is a narrow band device by nature, despite its modest size [2]. The bandwidth of the balun can be expanded by adding more half-wavelength transmission lines [3]. On the other hand, microwave circuits will require a lot of space for this design. Distributed baluns additionally include linked line and parallel plate baluns [4-6]. A few of these distributed-element baluns necessitate multilayer or nonplanar structures, which add to the complexity of the design. Lumped elements can also be used in the design of the baluns. Low frequency and MMIC applications are best served by lumped-element baluns, which can be used as low-pass and high-pass filter architectures [7], [8].

The hybrid rat-race ring serves as the foundation for lumped-element balun theory. Lumped component representations substitute the distributed transmission lines in the rat-race ring circuit. The lumped element low-pass filter networks take the role of the rat-race ring's quarter wavelength lines. A high-pass filter network takes the role of the three-quarter wavelength line [2]. These baluns require a lot of lumped parts. The third balun arrangement was presented in [9]–[11] and comprises of both lumped and dispersed parts. These baluns' derivations require electromagnetic simulations [10], parametric analysis [11], or experimental techniques.

The current study outlines a distributed-element balun constructed through the analysis of even- and odd-mode behavior in a 3-port network. This technique outlines the odd and even mode criteria for 4-port symmetrical networks, providing crucial understanding for synthesizing and designing these balun structures. The research will delve into creating novel balun architectures and precise design formulas specifically tailored for the operating frequency of this balun category.

## 2. Theory and Analysis

As seen in Figure 1, the origin of the balun is the symmetrical four-port network, where one port is concluded with an open circuit, a three-port device that is given here. An unbalanced input with source impedance $Z_{in}$ will be converted into balanced outputs with load impedances $Z_{out}$ by the balun.

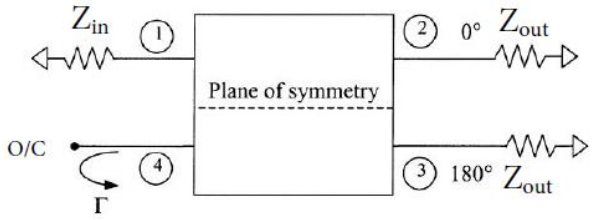


Figure 1: A balanced four-port network with one port concluded.

$Z_{in}$ and $Z_{out}$ are equal impedances. As a result, the balun has no effect on the source's and load's impedance. The 3-port network must satisfy these conditions to function as a balun

$$S_{21} = -S_{31} \quad (1)$$

$$S_{11} = 0 \quad (2)$$

Assuming that the even-mode transmission coefficient $T_{even}$ and the odd-mode impedance $Z_{odd}$ are obtained using equation 3 and 4, ideal signals exhibiting identical amplitudes and inverted phases at the balanced output terminals ($S_{21} = -S_{31}$) alongside effective input alignment ($S_{11} = 0$) at the balun's input

$$T_{even} = 0 \quad (3)$$

$$Z_{odd} = 2\,Z_0 \quad (4)$$

The circuit diagram of the balun shown in Figure 2 undergoes examination using even- and odd-mode analysis techniques in order to realize equations 3 and 4. The suggested balun is made up of four transmission lines with impedances $Z_2$ and an electrical length $\theta_2$ in series , along with four transmission lines of impedances $Z_1$ and $Z_3$ and electrical lengths $\theta_1$ and $\theta_3$ arranged in parallel. A transmission line, open at one end and holding an impedance of $\frac{Z_1}{2}$, featuring an electrical length of $\left(\frac{\pi}{2} - \theta_1\right)$ , is connected in parallel with shunted lines close to port one, or P1.

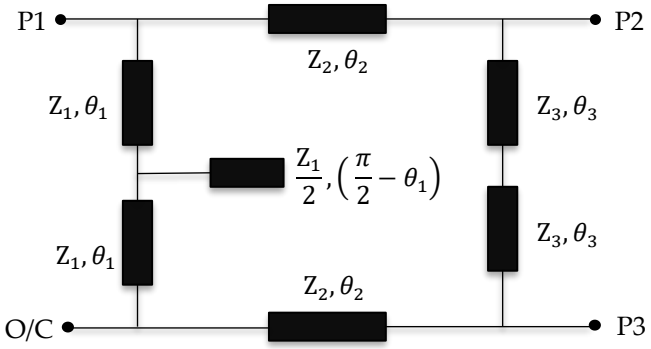


Figure 2: Illustration outlining the suggested three-port balun circuit.

2.1 Analysis of Even-Mode Characteristics of The Balun Circuit

Due to the symmetrical nature of the balun design shown in Figure 3, the symmetry plane effectively transforms into a simulated open circuit. The two sections of the open-ended transmission line are made up of impedances $Z_1$ and electrical lengths $\left(\frac{\pi}{2} - \theta_1\right)$. At port P1, a single transmission line with impedance $Z_1$ and electrical length $\frac{\pi}{2}$ is created by merging two transmission lines having impedances $Z_1$ and electrical lengths $\theta_1$ and $\left(\frac{\pi}{2} - \theta_1\right)$. According to transmission line theory, the input impedance of a terminated transmission line at the generator position $z = -L$, is as follows:

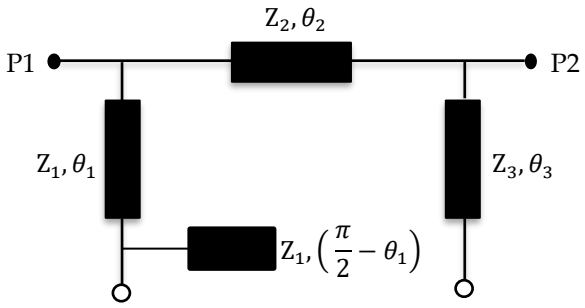


Figure 3: Even-mode configuration of the suggested balun circuit.

$$Z_{in} = Z_{(z=-L)} = Z_0 \frac{Z_L + Z_0 \tanh \gamma L}{Z_0 + Z_L \tanh \gamma L} \quad (5)$$

The input impedance for a lossless transmission line becomes

$$Z_{in} = Z_0 \frac{Z_L + jZ_0 \tanh \beta L}{Z_0 + jZ_L \tanh \beta L} \quad (6)$$

In a particular case of a terminated transmission line's input impedance when one terminal is left unconnected, equation 6 can be streamlined to:

$$Z_{in}|_{Z_L \to \infty} = -jZ_0 \cot(\beta L) \quad (7)$$

The behavior of a transmission line at various wavelengths ($\lambda$) for a given length affects the input impedance $Z_{in}$ in the following ways:

- When the length of the transmission line is an odd multiple of $\lambda/4$ (e.g., $\lambda/4$, $3\lambda/4$, $5\lambda/4$, ...), the open circuit at the far end appears as a short circuit at the input, resulting in a zero-input impedance.
- When the length of the transmission line is an even multiple of $\lambda/2$ (e.g., $\lambda/2$, $\lambda$, $3\lambda/2$, ...), the open circuit at the far end appears as an open circuit at the input, leading to an infinite input impedance.

Since the product of the phase constant ($\beta$) and the length ($L$) is equal to $\pi/2$ in equation 7, the input impedance of an open-ended transmission line at port one in the circuit depicted in Figure 4 is zero. This means that, under these conditions, the transmission line appears as a short circuit at P1, and the input impedance $Z_{in}$ of the related even-mode half-circuit is nil, causing zero power transmission to P2, leading to a corresponding zero value for the transmission coefficient $T_{even}$.

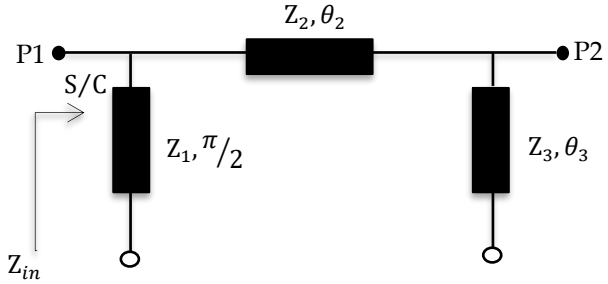


Figure 4: Even-mode configuration of the balun featuring a short circuit at P1.

2.2 Analysis of Odd-Mode Characteristics of The Balun Circuit

The corresponding odd-mode half-circuit of the balun is linked to the ground as shown in Figure 5 because the odd symmetry of the balun circuit causes the plane of symmetry to become a virtual short. Equation 4 demonstrates that when dealing with a short-circuit situation the odd-mode impedance should be double the characteristic impedance $Z_0$ of the odd-mode circuit to attain complete alignment at the balun input. The three transmission line sections in Figure 6 are treated as a single transmission line with impedance $Z_0 = 70.70\ \Omega$ and electrical length $\theta = \pi/2$, since the impedances and electrical lengths of the two parallel transmission lines are presumed to be identical. Known by most as a quarter wavelength transmission line, this transmission line performs the following impedance transformation between the input and output

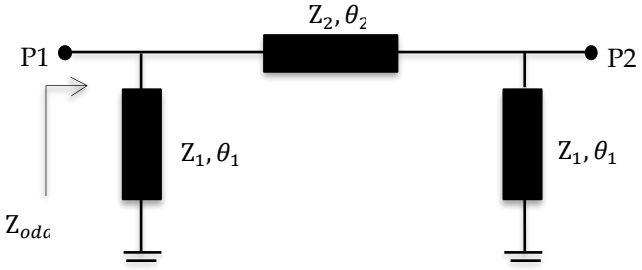


Figure 5: Odd-mode configuration of the suggested balun circuit.

$$Z_{in} = \frac{Z_0^2}{Z_L} \tag{8}$$

This expression will result in the odd-mode impedance being

$$Z_{odd} = \frac{Z_T^2}{Z_L} \tag{9}$$

Comparing equations 8 and 9, the equivalent transmission line of impedance $Z_T$ must be the same as the quarter wavelength transmission line of impedance $Z_o$. As a result, the ABCD matrix of the quarter-wavelength line needs to align with the combined sum of the ABCD matrices of the three transmission lines within the odd-mode circuit.

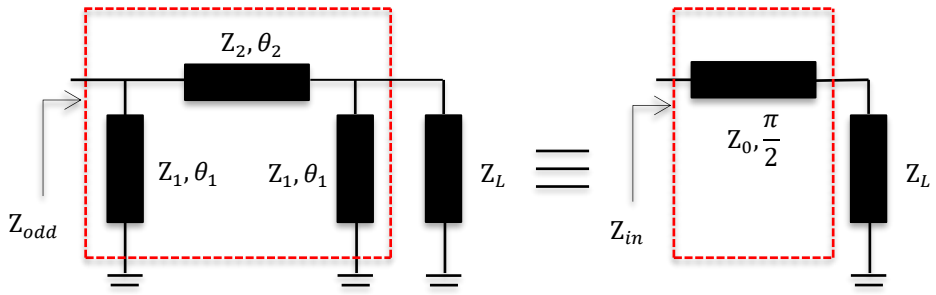


(a) (b)

Figure 6: (a) Odd-mode configuration of the suggested balun circuit, (b) Quarter-wavelength transmission line.

Two shunt transmission lines form an ABCD matrix as follow:

$$\begin{bmatrix} 1 & 0 \\ -j\frac{1}{Z_1 \tan\theta_1} & 1 \end{bmatrix} \tag{10}$$

The series transmission line's ABCD matrix is

$$\begin{bmatrix} \cos\theta_2 & j\,Z_2\,\sin\theta_2 \\ j\frac{1}{Z_2}\sin\theta_2 & \cos\theta_2 \end{bmatrix} \tag{11}$$

The above matrices multiplied from left to right yields the total ABCD matrix

$$\begin{bmatrix} 1 & 0 \\ -j\frac{1}{Z_1 \tan\theta_1} & 1 \end{bmatrix} * \begin{bmatrix} \cos\theta_2 & j\,Z_2\,\sin\theta_2 \\ j\frac{1}{Z_2}\sin\theta_2 & \cos\theta_2 \end{bmatrix} * \begin{bmatrix} 1 & 0 \\ -j\frac{1}{Z_1 \tan\theta_1} & 1 \end{bmatrix} =$$

$$\begin{bmatrix} \cos\theta_2 + \frac{Z_2\,\sin\theta_2}{Z_1\,\tan\theta_1} & j\,Z_2\,\sin\theta_2 \\ j\left(\frac{\sin\theta_2}{Z_2} - \frac{2\,\cos\theta_2}{Z_1\,\tan\theta_1} - \frac{Z_2\,\sin\theta_2}{Z_1^2\,\tan\theta_1{}^2}\right) & cos\,\theta_2 + \frac{Z_2\,sin\,\theta_2}{Z_1\,tan\,\theta_1} \end{bmatrix} \tag{12}$$

The quarter wavelength's ABCD matrix with a characteristic impedance $Z_0 = 70.7\ \Omega$ is

$$\begin{bmatrix} 0 & j\,70.7 \\ j\,0.014 & 0 \end{bmatrix} \tag{13}$$

There are four equations if the two matrices, 12 and 13, are equal.

$$\begin{bmatrix} \cos\theta_2 + \frac{Z_2\ \sin\theta_2}{Z_1\ \tan\theta_1} & j\,Z_2\ \sin\theta_2 \\ j\left(\frac{\sin\theta_2}{Z_2} - \frac{2\ \cos\theta_2}{Z_1\ \tan\theta_1} - \frac{Z_2\ \sin\theta_2}{Z_1^2\ \tan{\theta_1}^2}\right) & cos\,\theta_2 + \frac{Z_2\ sin\,\theta_2}{Z_1\ tan\,\theta_1} \end{bmatrix} = \begin{bmatrix} 0 & j\,70.7 \\ j\,0.014 & 0 \end{bmatrix} \tag{14}$$

$$cos\,\theta_2 + \frac{Z_2\ sin\,\theta_2}{Z_1\ tan\,\theta_1} = 0 \tag{15}$$

$$Z_2\ sin\,\theta_2 = 70.7 \tag{16}$$

$$\frac{sin\,\theta_2}{Z_2} - \frac{2\ cos\,\theta_2}{Z_1\ tan\,\theta_1} - \frac{Z_2\ sin\,\theta_2}{Z_1^2\ tan{\theta_1}^2} = 0.014 \tag{17}$$

$$cos\,\theta_2 + \frac{Z_2\ sin\,\theta_2}{Z_1\ tan\,\theta_1} = 0 \tag{18}$$

Through the solution of these four equations, the final result is provided as

$$\theta_1 = \tan^{-1}(-b)\,, \theta_2 = \tan^{-1}(a) \tag{19}$$

$$Z_1 = 70.7 * \frac{\sqrt{1+a^2}}{b}, Z_2 = 70.7 * \frac{\sqrt{1+a^2}}{a} \tag{20}$$

where $a$ and $b$ are real numbers.

The design constraints stem from the ranges of $Z_1$and $Z_2$, which should fall between 20 Ω and 120 Ω. Accordingly, the value of $\theta_2$ should range from 36 and 89 degrees. For each value of $\theta_2$, there exist multiple values of $\theta_1$.

## 3. Design and Simulation

As discussed in the preceding section, Figure 7 illustrates the newly proposed balun's layout. Both of the limitations in equations 3 and 4 are met by the three-port balun, which was created by converting the four-port network. It achieves a transmission stop within the even-mode configuration as the impedance $Z_{even}$ approaches zero, and it attains satisfactory alignment within the odd-mode configuration when the impedance $Z_{odd}$ matches twice the input termination

impedance. The balun comprises two parallel transmission lines of impedance 49.5 Ω and electrical length 178°, two series transmission lines of impedance 70.70 Ω and electrical length 92°, and one open-ended termination of impedance 25 Ω and electrical length 92°. The balun's three ports each have an impedance of 50 Ω.

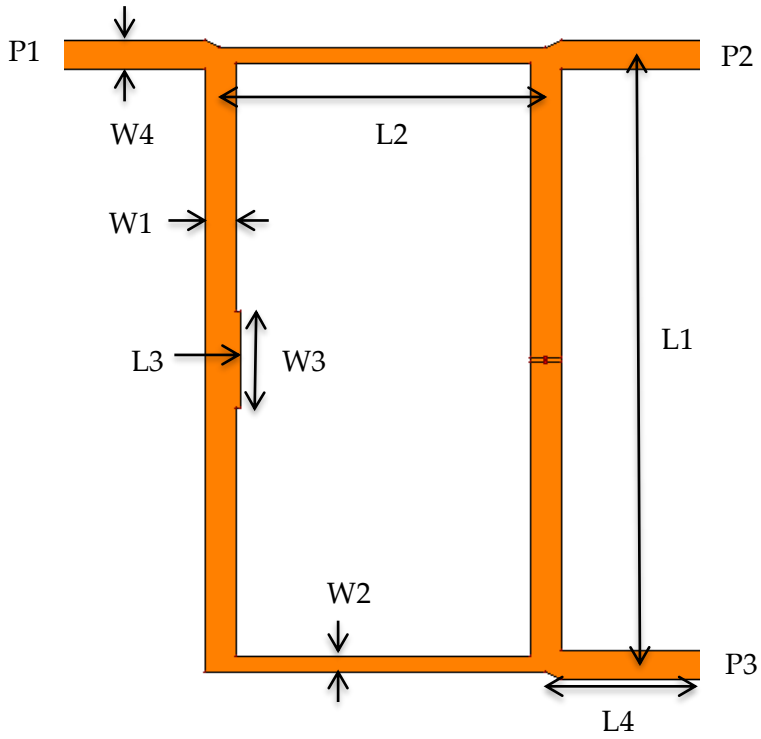


Figure 7: Topology of the proposed balun.

The transmission lines' lengths and widths have been determined and recorded in Table 1. Using HFSS, the proposed balun has been designed and simulated. Figure 7 illustrates the configuration of this three-port balun with terminations connected to 50 Ω loads. The frequency responses of the proposed balun are presented in Figure 8 through simulation. The frequency center is 2.4 GHz, the insertion loss ranges from 3 dB with a tolerance of ± 0.76 dB, and the return loss remains below -10 dB across the entire bandwidth, and the 3-dB fractional bandwidth is 40%. Figure 9 illustrates how, throughout the design frequency range, The balun exhibits a phase difference of 180 degrees between ports two and three.

Table 1. The balun's dimensions (unit: millimeter).

| Parameter | 1 | 2 | 3 | 4 |
|---|---|---|---|---|
| Length (L) | 38 | 19.8 | 1.2 | 10 |
| Width (W) | 1.9 | 1 | 4.9 | 1.8 |

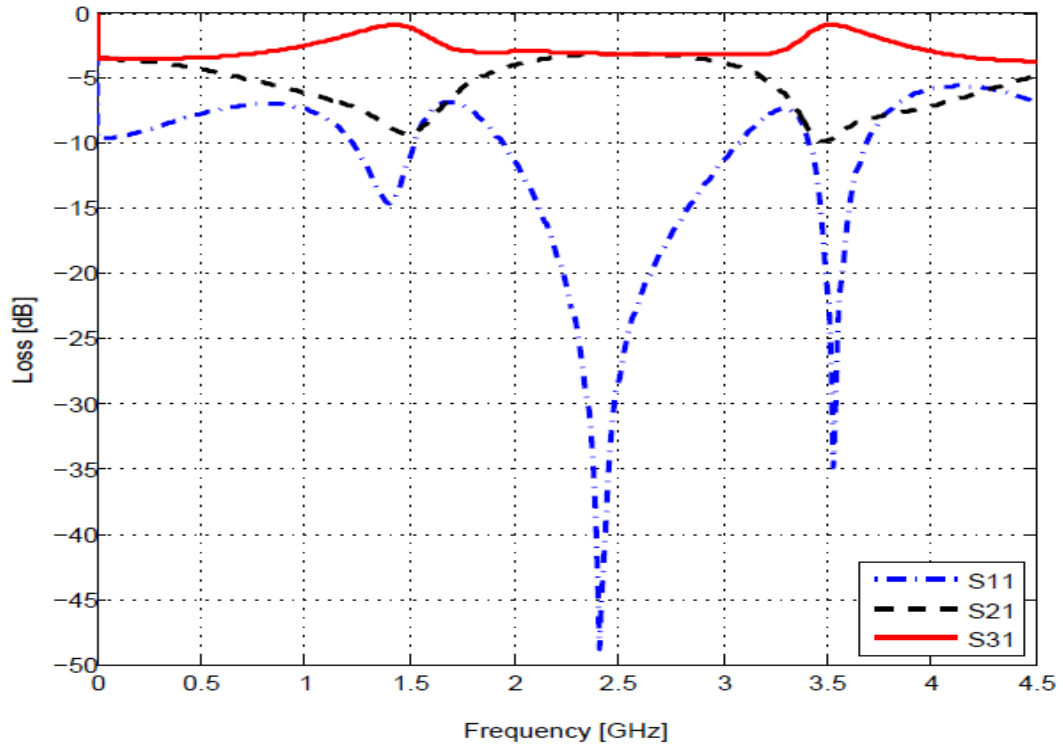


Figure 8: Simulation results for the balun's return loss and insertion loss.

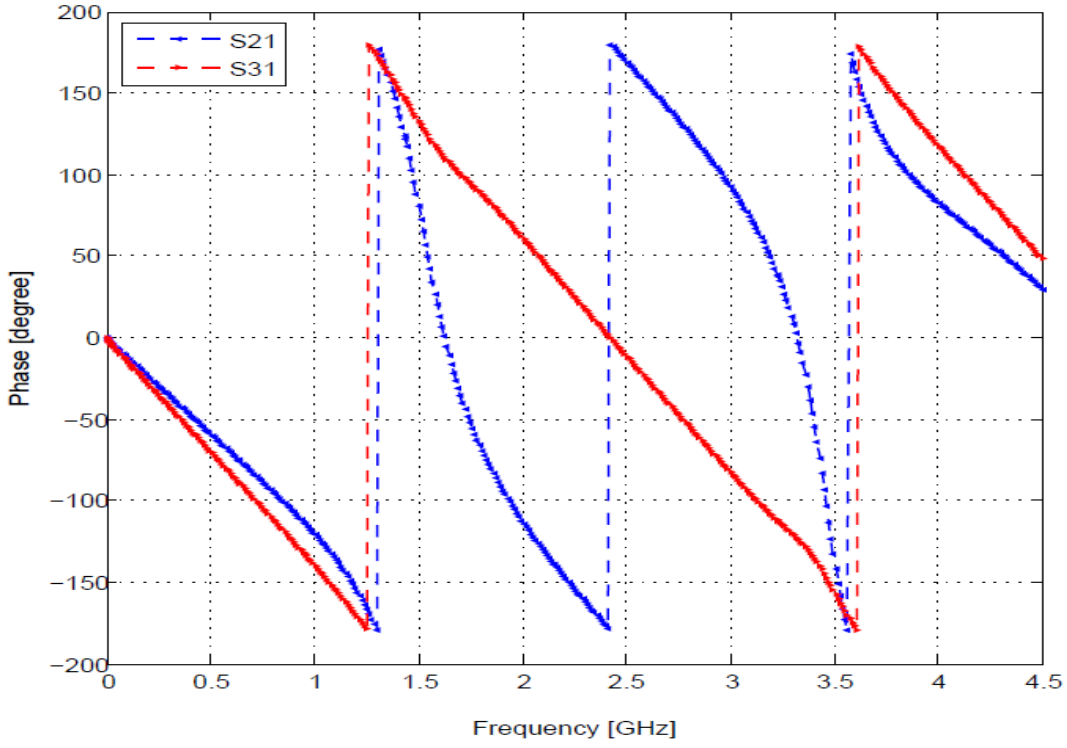


Figure 9: Simulation results of phase response of the balun.

## 4. Fabrication and Measurements

In order to validate the design idea, the proposed balun has been integrated into the microstrip configuration on the RO4003 substrate (metal thickness = 17 $\mu$m, loss tangent ($\delta$) = 0.002, dielectric constant ($\varepsilon_r$) = 3.38, and substrate thickness ($h$) = 0.813 mm). Its circuit dimensions are 77 mm by 39 mm. There is two-sided metallization. The balun and a microstrip feed form the top metallization. As seen in Figure 10, The metal layer on the lower plane is a truncated microstrip ground. Figures 10 and 11, respectively, display the measured results of the balun's phase response, insertion loss, and return loss. With the E5063A ENA vector network analyzer, the three-port balun's measurements are obtained.

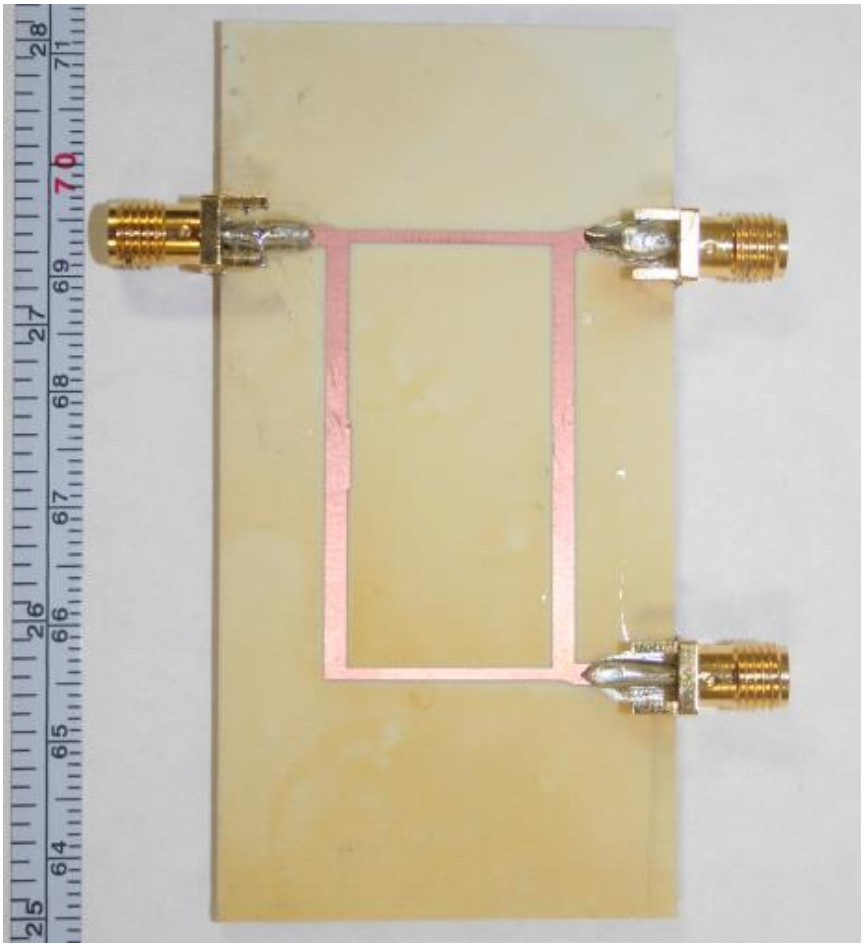

Figure 10: Photograph of proposed balun.

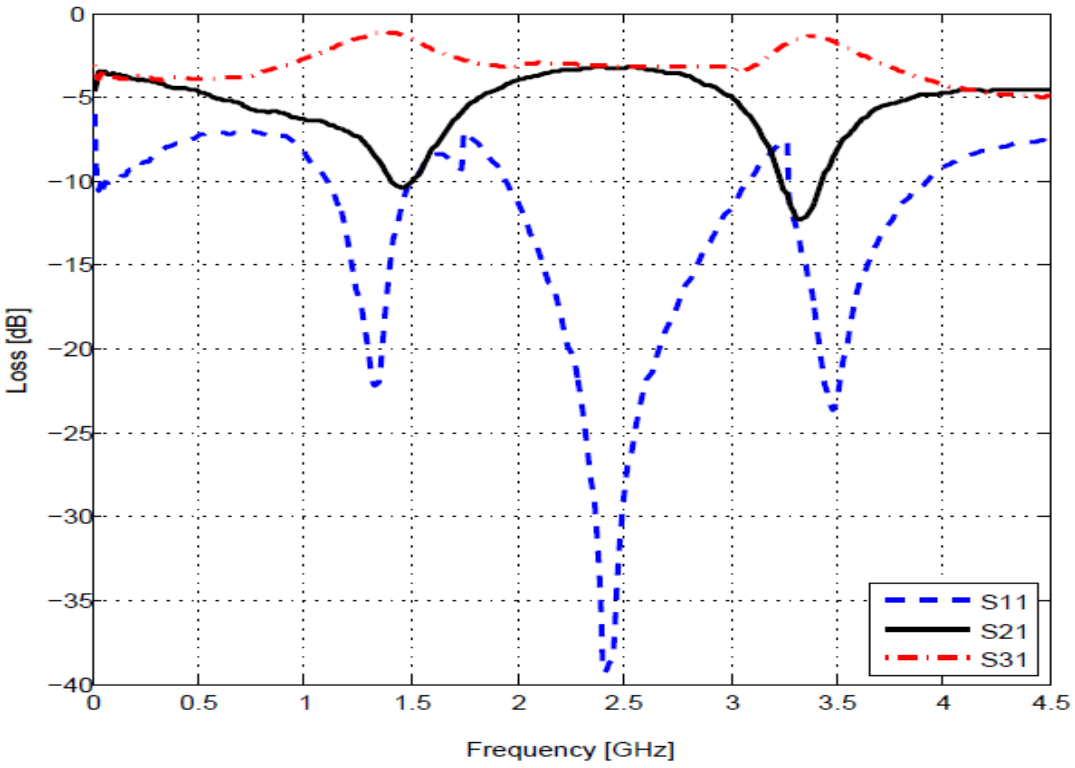


Figure 11: Measurement outcomes of insertion loss and return loss.

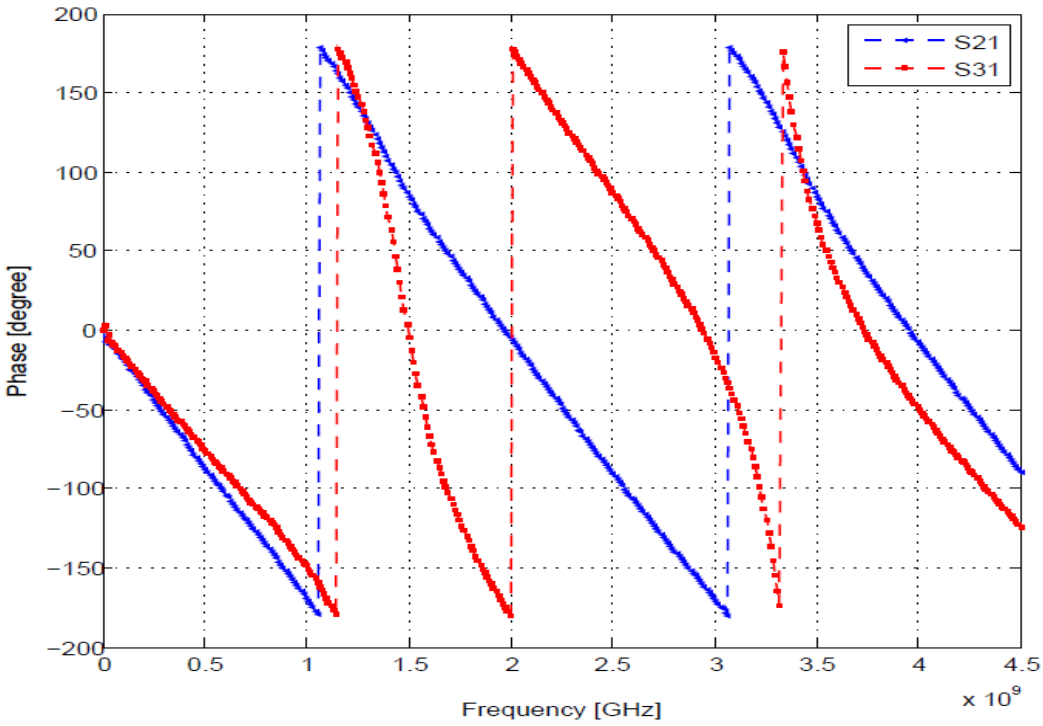


Figure 12: Measurement outcomes of phase characteristics of the balun.

## 5. Conclusion

An entirely innovative three-port balun, converting between balanced and unbalanced configurations, has been introduced. Many wireless and microwave systems, including antennas, balanced amplifiers, and mixers, use baluns. There has also been discussion of the precise design processes and measured outcomes. With equal amplitudes and 180 phase differences, this balun produces perfectly balanced signals at the output ports. Port one also exhibits good impedance matching. The operating frequency of the balun is 2.4 GHz. The performance of the indicated balun, as demonstrated by the fabrication and measurement of experimental prototypes, closely resembles the design concept.

## References

[1] B Mayer and R Knoechel, "Biasable balanced mixers and frequency doublers using a new planar balun," Conference Proceeding: 20th European Microwave Conference, V2, pp. 1027-1032, 1990.

[2] R. Sturdivant, "Balun design for wireless, mixers amplifiers, and antennas," Appl. Microwaves, vol. 5, pp. 34-44, Summer 1993.

[3] D. Raicu, "Design of planar, single-layer microwave baluns," in IEEE MTT-S Int. Microwave symp. Dig, pp. 801-804, 1998.

[4] B. Climer, "Analysis of suspended microstrip taper baluns," Proc. IEE, Vol. 135, Pt H, No. 2, pp. 65-69, April 1988.

[5] A. M. Pavio and A. Kikel, "A monolithic or hybrid broadband compensated balun," in IEEE MTT-S Int. Microwave symp. Dig, pp. 483-486, 1990.

[6] Y. C. Leong, K. S. Ang, and C. H. Lee, "A derivation of a class of 3-port baluns from symmetrical 4-port networks," IEEE MTT-S Digest, pp. 1165-1168, 2002.

[7] H. K. Chiou, H. H. Lin, and C. Y. Chang, "Lumped-element compensated high/low-pass balun design for MMIC double-balanced mixer", IEEE Microwave Guided Wave Lett., vol. 7, pp. 248-250, Aug. 1997.

[8] Samuel J. Parisi, "Monolithic, lumped element, single sideband modulator," IEEE MTT-S International Microwave Symp. Dig., pp. 1047-1050, 1992.

[9] K. S. Ang, Y. C. Leong, and C. H. Lee, "Analysis and design of miniaturized lumped-distributed impedance-transforming baluns," IEEE Transactions on Microwave Theory and Techniques, vol. 51, no. 3, March 2003.

[10] C. W. Tang and C. Y. Chang, "A semi-lumped balun fabricated by low temperature co-fired ceramic," in IEEE MTT-S Int. Microwave Symp. Dig., pp. 2201–2204, 2002.

[11] B. P. Kumar, G. R. Branner, and B. Huang, "Parametric analysis of improved planar balun circuits for wireless microwave and RF applications," in Proc. IEEE Midwest Circuits and Systems Symp., pp. 474–475, 1998.